CHAPTER 4

MODES OF PHOTONIC MOLECULES AS OPTICALLY COUPLED CIRCULAR RESONATORS

A great attention is paid lately in theoretical and experiments photonics to the fabrication and investigation of the ordered structures composed of several dielectric microresonators. As known, since some time ago a term “photonic crystal” has obtained a wide circulation. It relates to the infinite-periodic structures composed of microparticles; the optical properties of such structures have many common features with the quantum-mechanical properties of lattices of atoms in crystals. Therefore, by analogy with atoms and molecules the stand-alone microresonators are sometimes called “photonic atoms,” and the structures made of several such resonators became known as “photonic molecules” [42–44, 161,162].

The photonic molecules are attractive by many reasons. For example, although the microdisk laser working on the whispering-gallery modes are famous for the ultra-low thresholds, they have small output power. Uniting several microdisks in a photonic molecule may help raise the output power. However, when designing such lasers, an accurate account of the interference of the fields radiated by each of the disks becomes crucial.

Similarly to the disk encased in a circular reflector (see Chapter 3), any photonic molecule consists of several partial regions having different refractive indices. As the regions boundaries are partially transparent, the natural modes of these regions are optically coupled and therefore the term “supermode” is used.

The investigation of the supermodes of photonic molecules by the methods of boundary-value problems for the Maxwell equations and computational electromagnetics is a complicated and timely problem. There are several papers where the supermodes of *passive* photonic molecules have been studied and corresponding complex frequencies, Q-factors, and natural fields have been computed as a function of geometrical and material parameters [163].

This Chapter deals with the study of lasing spectra and thresholds for the supermodes of the cyclic photonic molecules composed of the active circular resonators whose centers are located in the corners of regular polygons. This study is performed in the framework of the lasing eigenvalue problem formulation. Considered are also the ways of improvement of directionality of emission for the twin-disk photonic molecule, relatively to the emission from a stand-alone disk laser.

4.1. Supermodes of two identical active resonators

In this subsection, we study the lasing spectra and thresholds and also the directionalities of emission for the supermodes of photonic molecules made of two identical active thin microdisks. In Fig. 4.1, presented is a 3-D geometry of such a photonic molecule: two identical microdisks of radius a are made of non-magnetic material with the refractive index α in the absence of pumping and $\nu = \alpha - i\gamma$ under the pumping. The rim-to-rim distance (air gap) between the disks is denoted as w.

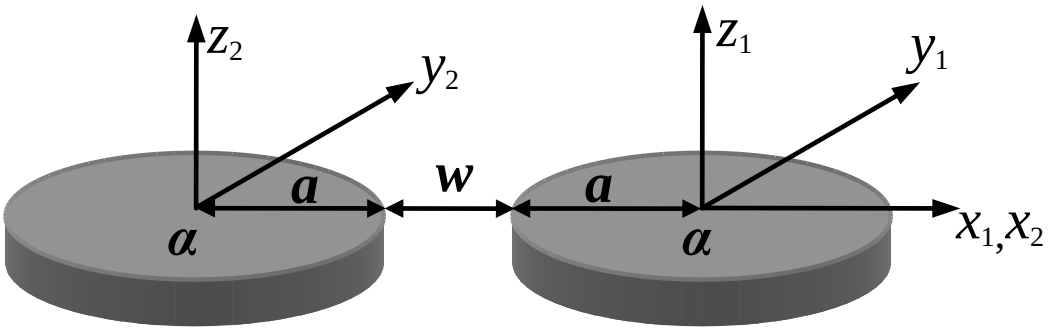

Fig. 4.1 Photonic molecule composed of two identical microdisks

As before, we will assume that the 3-D problem for the electromagnetic field in the presence of two thin disks has been already reduced, using the effective refractive index method (see section 2.1), to a 2-D problem with conditions (2.8), (2.12) – (2.13), (2.15). Fig. 4.2 depicts the 2-D model of the photonic molecule made of twin circular resonators. We will further consider only the case of the H-polarization, so that the field function is $U(\rho,\varphi) = H_z$. As such a photonic molecule is made of the

circular resonators the separation of variables in the local polar coordinates enables one to reduce the lasing eigenvalue problem to an infinite-matrix equation.

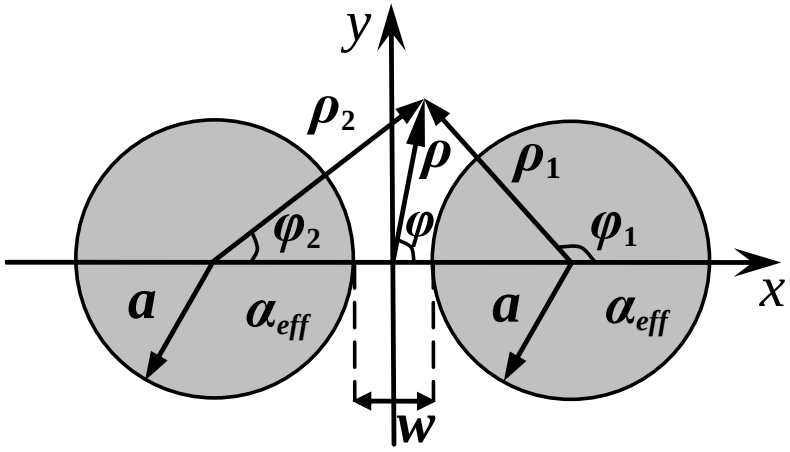

Fig. 4.2 Two-dimensional model of a photonic molecule made of two identical optically coupled circular resonators

Introduce two local systems of polar coordinates, (ρ_1,φ_1) and (ρ_2,φ_2), in such a way that each of them has the origin at the center of one of the resonators, and also the global coordinates, (x,y) and (ρ,φ), with the origin at the crossing of the lines of symmetry, i.e. the *x* and *y* axes (see Fig. 4.2). In line with the method of separation of variables, represent the field in each of three domains as a series in terms whose terms satisfy the Helmholtz equation, condition of local power finiteness, and condition of radiation,

$$\rho_1 < a_1: \qquad U(\rho_1,\varphi_1) = \sum_{p=-\infty}^{\infty} A_p J_p(k\nu\rho_1) e^{ip\varphi_1},$$

$$\rho_2 < a_2: \qquad U(\rho_2,\varphi_2) = \sum_{p=-\infty}^{\infty} B_p J_p(k\nu\rho_2) e^{ip\varphi_2}, \tag{4.1}$$

$$(\rho_1 > a_1) \wedge (\rho_2 > a_2): U(\rho,\varphi) = \sum_{p=-\infty}^{\infty} C_p H_p^{(1)}(k\rho_1) e^{ip\varphi_1} + \sum_{p=-\infty}^{\infty} D_p H_p^{(1)}(k\rho_2) e^{ip\varphi_2},$$

where J_p and $H_p^{(1)}$ are the Bessel and Hankel functions, $\nu = \alpha_{eff} - i\gamma$ is the complex refractive index of circular resonators, $k = \omega / c$ is the wavenumber, c is the light velocity, w is the frequency, and $\{A_p, B_p, C_p, D_p\}_{p=-\infty}^{\infty}$ are unknown coefficients.

Further, substitute (4.1) into the boundary conditions (2.12) and use the addition theorem for the cylindrical functions (see [160] or [164]) to obtain the following set of the linear algebraic equations

$$\begin{aligned}
&\sum_{p=-\infty}^{\infty} A_p J_p(\kappa\nu) e^{ip\varphi_1} - \sum_{p=-\infty}^{\infty} C_p H_p^{(1)}(\kappa) e^{ip\varphi_1} - \sum_{p=-\infty}^{\infty} D_p \sum_{n=-\infty}^{\infty} J_n(\kappa) H_{n-p}^{(1)}(\kappa l) e^{in\varphi_1} = 0,\\
&\sum_{p=-\infty}^{\infty} B_p J_p(\kappa\nu) e^{ip\varphi_2} - \sum_{p=-\infty}^{\infty} D_p H_p^{(1)}(\kappa) e^{ip\varphi_2} - \sum_{p=-\infty}^{\infty} C_p \sum_{n=-\infty}^{\infty} J_n(\kappa) H_{p-n}^{(1)}(\kappa l) e^{in\varphi_2} = 0,\\
&\nu^{-1} \sum_{p=-\infty}^{\infty} A_p J_p'(\kappa\nu) e^{ip\varphi_1} - \sum_{p=-\infty}^{\infty} C_p H_p'^{(1)}(\kappa) e^{ip\varphi_1} - \sum_{p=-\infty}^{\infty} D_p \sum_{n=-\infty}^{\infty} J_n'(\kappa) H_{n-p}^{(1)}(\kappa l) e^{in\varphi_1} = 0,\\
&\nu^{-1} \sum_{p=-\infty}^{\infty} B_p J_p'(\kappa\nu) e^{ip\varphi_2} - \sum_{p=-\infty}^{\infty} D_p H_p'^{(1)}(\kappa) e^{ip\varphi_2} - \sum_{p=-\infty}^{\infty} C_p \sum_{n=-\infty}^{\infty} J_n'(\kappa) H_{p-n}^{(1)}(\kappa l) e^{in\varphi_2} = 0,
\end{aligned} \tag{4.2}$$

where $\kappa = ka$ is the normalized frequency, $l = 2 + w/a$ is the normalized distance between the centers of circular resonators (as we will see further, they should not touch each other: $w > 0$), and the prime denotes the differentiation in argument.

Multiplying each equation in (4.2) with function $e^{im\varphi}$, integrating the product in φ over $[0, 2\pi]$, and taking account of the orthogonality of trigonometric functions in the space of integrable functions $L_2[0, 2\pi]$, we arrive at

$$\begin{aligned}
&A_{-m} J_m(\kappa\nu) - C_{-m} H_m^{(1)}(\kappa) - \sum_{p=-\infty}^{\infty} (-1)^{m+p} D_p J_m(\kappa) H_{m+p}^{(1)}(\kappa l) = 0,\\
&B_{-m} J_m(\kappa\nu) - D_{-m} H_m^{(1)}(\kappa) - \sum_{p=-\infty}^{\infty} C_p J_m(\kappa) H_{m+p}^{(1)}(\kappa l) = 0,
\end{aligned}$$

$$\begin{aligned} \nu^{-1}A_{-m}J'_m(\kappa\nu) - C_{-m}H'^{(1)}_m(\kappa) - \sum_{p=-\infty}^{\infty}(-1)^{m+p}D_pJ'_m(\kappa)H^{(1)}_{m+p}(\kappa l) = 0, \\ \nu^{-1}B_{-m}J'_m(\kappa\nu) - D_{-m}H'^{(1)}_m(\kappa) - \sum_{p=-\infty}^{\infty}C_pJ'_m(\kappa)H^{(1)}_{m+p}(\kappa l) = 0, \end{aligned} \tag{4.3}$$

where $m = 0,\pm1,\pm2\ldots$. However, the set of matrix equations (4.3) is not favorable for computations. Using some algebraic transformations and excluding two sets of unknown coefficients, $\{C_p, D_p\}_{p=-\infty}^{\infty}$,one can reduce it to the following set:

$$\begin{cases} A_{-m}F_m(\kappa,\gamma)J_m(\kappa) + \sum_{p=-\infty}^{\infty}(-1)^{m+p}B_pJ_m(\kappa)V_p(\kappa,\gamma)H^{(1)}_{m+p}(\kappa l) = 0, \\ B_{-m}F_m(\kappa,\gamma)J_m(\kappa) + \sum_{p=-\infty}^{\infty}A_pJ_m(\kappa)V_p(\kappa,\gamma)H^{(1)}_{m+p}(\kappa l) = 0, \end{cases} \tag{4.4}$$

where

$$\begin{aligned} F_m(\kappa,\gamma) &= J_m(\kappa\nu)H'^{(1)}_m(\kappa) - \nu^{-1}J'_m(\kappa\nu)H^{(1)}_m(\kappa), \\ V_m(\kappa,\gamma) &= J_m(\kappa\nu)J'_m(\kappa) - \nu^{-1}J'_m(\kappa\nu)J_m(\kappa) \end{aligned} \tag{4.5}$$

The expansion coefficients of the field out of the resonators can be expressed via the expansion coefficients of the field inside the resonators as

$$C_{-m} = -\frac{\pi\kappa}{2i}A_{-m}V_m(\kappa,\gamma), \quad D_{-m} = -\frac{\pi\kappa}{2i}B_{-m}V_m(\kappa,\gamma) \tag{4.6}$$

Finally, on making the substitution $m \to -m$ and introducing new unknowns as

$$x_m = A_mF_m(\kappa,\gamma)J_m(\kappa); \quad y_m = B_mF_m(\kappa,\gamma)J_m(\kappa), \tag{4.7}$$

we obtain the following pair of coupled matrix equations:

$$\begin{cases} x_m + \sum\limits_{p=-\infty}^{\infty} y_p \dfrac{J_m(\kappa)V_p(\kappa,\gamma)}{F_p(\kappa,\gamma)J_p(\kappa)} H_{m-p}^{(1)}(\kappa l) = 0, \\ \\ y_m + \sum\limits_{p=-\infty}^{\infty} x_p \dfrac{J_m(\kappa)V_p(\kappa,\gamma)}{F_p(\kappa,\gamma)J_p(\kappa)} H_{p-m}^{(1)}(\kappa l) = 0, \quad m = 0, \pm 1, \pm 2, ... \end{cases} \tag{4.8}$$

In the operator notation, the set (4.8) take form of a single equation with a block-type (2×2) matrix operator U,

$$(I+U)Z = 0, \quad U = \begin{pmatrix} 0 & U^{(1)} \\ U^{(2)} & 0 \end{pmatrix}, \qquad Z = (..., x_{-1}, x_0, x_1, ..., y_{-1}, y_0, y_1, ...), \tag{4.9}$$

where the matrix elements of the off-diagonal blocks are given by

$$U_{mp}^{(1)} = \frac{V_p(\kappa,\gamma)J_m(\kappa)}{F_p(\kappa,\gamma)J_p(\kappa)} H_{m-p}^{(1)}(\kappa l), \quad U_{mp}^{(2)} = \frac{V_p(\kappa,\gamma)J_m(\kappa)}{F_p(\kappa,\gamma)J_p(\kappa)} H_{p-m}^{(1)}(\kappa l), \tag{4.10}$$

and $I = \{\delta_{mp}\}_{m,p=-\infty}^{\infty}$ is the identity matrix operator.

Let us verify the behavior of the matrix elements (4.10) if $m, p \to \infty$. To this end, we use asymptotics of cylindrical functions for large integer orders [156, 160]:

$$J_n(z) \sim \frac{(z/n)^n}{n!}, \quad H_n^{(1)}(z) \sim -\frac{i}{\pi}(n-1)!(z/2)^{-n}, \quad n \to \infty \tag{4.11}$$

On substituting (4.11) into (4.10), we arrive at the expression

$$U_{mp}^{(1,2)} \sim const \frac{1}{l^{|p|+|m|}} \frac{(|p|+|m|)!}{|p|!|m|!}, \tag{4.12}$$

from which it follows that so far as $l > 2$, then $\sum_{m,p=-\infty}^{\infty} |U^2| < \infty$ (see [164], p. 236).

Hence, the infinite-dimensional equation (4.8) is a Fredholm second kind operator equation, and its determinant exists as a function of parameters. Therefore, the lasing eigenvalue problem is reduced to the search for the roots of infinite-order determinantal equation,

$$\det[I + U(\kappa, \gamma)] = 0 \qquad (4.13)$$

One can show that there is a one-to-one correspondence between the eigenvalues (κ, γ) of original lasing eigenvalue problem and the roots of (4.13). As the set (4.8) is of the Fredholm type, the roots of truncated determinantal equations having finite-order blocks $2N \times 2N$ converge to the exact roots of infinite-order determinantal equation if the truncation order grows, $N \to \infty$. The approximate roots can be found using various numerical techniques. We have been finding them by the iterative secant method (a two-parameter Newton method). In the process of iterations, very important role is played by the nearness of the initial guess to the true value of the root we are looking for.

For numerical solution of (4.13), it is convenient to reduce the matrix size using the symmetry considerations across two lines of symmetry (see Fig. 4.3).

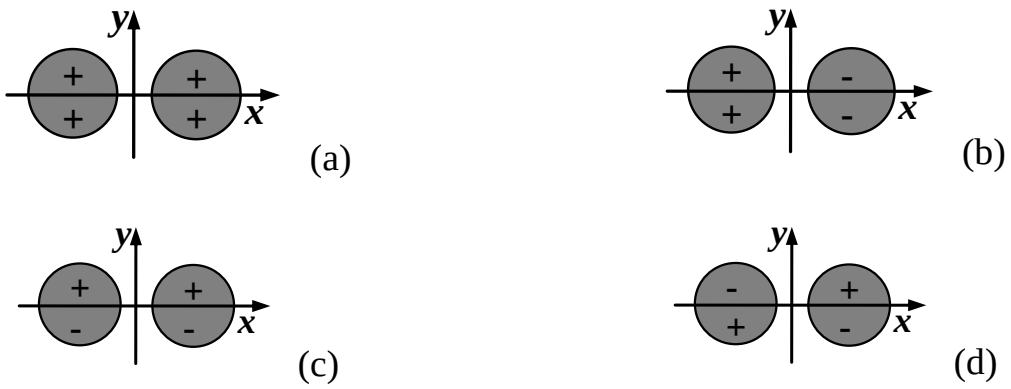

Fig. 4.3 Classes of symmetry for the modes in the twin-disk photonic molecule: (a) even field relatively to both x and y axes; (b) x-even and y-odd field; (c) x-odd and y-even field; and (d) odd field relatively to both x and y-axes.

All modes in the considered photonic molecule split into four orthogonal classes of symmetry, and for each class one can derive a separate matrix equation from (4.8). Here, one has to exploit the properties of symmetry (or anti-symmetry) of the field function U from (4.1) across the x and y-axes.

If the function U is odd with respect to the y-axis, then $C_p = -D_{-p}$ and $A_p = -B_{-p}$, and, according to (4.7), we have

$$y_{-p} = (-1)^{p+1} x_p . \tag{4.14}$$

If the function U is even with respect to the y-axis, then $C_p = D_{-p}$ and $A_p = B_{-p}$, and, according to (4.7), we have

$$y_{-p} = (-1)^{p} x_p . \tag{4.15}$$

If the function U is even with respect to the x-axis, then $A_p = (-1)^p A_{-p}$ and $B_p = (-1)^p B_{-p}$, and then from (4.7) it follows that

$$x_p = x_{-p}, \quad y_p = y_{-p} \tag{4.16}$$

If the function U is odd with respect to the x-axis, then $A_p = (-1)^{p+1} A_{-p}$ and $B_p = (-1)^{p+1} B_{-p}$, and from (4.7) it follows that

$$x_p = -x_{-p}, \quad y_p = -y_{-p} \tag{4.17}$$

Using expressions from (4.14) to (4.17), we derive from (4.8) four independent equations for each symmetry class. Namely, for the modes whose fields are even across the both axes (for brevity, *x*-even/*y*-even modes),

$$x_m + \sum_{p=0}^{\infty} \mu_p x_p \frac{J_m(\kappa)V_p(\kappa,\gamma)}{F_p(\kappa,\gamma)J_p(\kappa)}\left[H^{(1)}_{m+p}(\kappa l) + (-1)^p H^{(1)}_{m-p}(\kappa l)\right] = 0 \qquad (4.18)$$

For the modes whose fields are even across the *x*-axis and odd across the *y*-axis (*x*-even/*y*-odd modes),

$$x_m - \sum_{p=0}^{\infty} \mu_p x_p \frac{J_m(\kappa)V_p(\kappa,\gamma)}{F_p(\kappa,\gamma)J_p(\kappa)}\left[H^{(1)}_{m+p}(\kappa l) + (-1)^p H^{(1)}_{m-p}(\kappa l)\right] = 0 \qquad (4.19)$$

For the modes whose fields are odd across the *x*-axis and even across the *y*-axis (*x*-odd/*y*-even modes),

$$x_m + \sum_{p=1}^{\infty} x_p \frac{J_m(\kappa)V_p(\kappa,\gamma)}{F_p(\kappa,\gamma)J_p(\kappa)}\left[H^{(1)}_{m+p}(\kappa l) - (-1)^p H^{(1)}_{m-p}(\kappa l)\right] = 0 \qquad (4.20)$$

And finally for the modes whose fields are odd with respect to the both axes (*x*-odd/*y*-odd modes),

$$x_m - \sum_{p=1}^{\infty} x_p \frac{J_m(\kappa)V_p(\kappa,\gamma)}{F_p(\kappa,\gamma)J_p(\kappa)}\left[H^{(1)}_{m+p}(\kappa l) - (-1)^p H^{(1)}_{m-p}(\kappa l)\right] = 0 \qquad (4.21)$$

In (4.18),(4.19) $m = 0,1,2,3...$, and, if $p = 0$, then $\mu_0 = 1/2$, otherwise $\mu_{p>0} = 1$.

Twin-disk photonic molecule is the simplest of the cyclic photonic molecules. The nomenclature of the supermodes in a cyclic photonic molecule can be conveniently built, for simplicity, on the basis of the mode classification in a stand-alone circular resonator with additional indication to the symmetry class across the lines of symmetry (i.e. the *x* and *y*-axes for the twin-disk photonic molecule).

In Figs. 4.4 and 4.5, presented are the dependences of the lasing mode frequencies and associated thresholds on the normalized rim-to-rim distance between the disks in the photonic molecule, w/a, for the supermodes $H_{m,n}^{(M)e,e}$, $H_{m,n}^{(M)e,o}$, $H_{m,n}^{(M)o,e}$, $H_{m,n}^{(M)o,o}$ $(m=7, n=1)$, where the sub-indices m and n correspond to the number of the field variations in local azimuth and in local radius in each circular resonator, and the super-indices $(e/o),(e/o)$ correspond to the symmetry or anti-symmetry of the mode field with respect to the *x* and *y*-axes, respectively; the upper index (*M*) shows the number of elementary resonators composing the photonic molecule (in the considered case, $M=2$). We emphasize that we deal with the supermodes as the photonic molecule is built of several (here, two) circular resonators. In this case, the minimum sphere or the full volume of the corresponding open resonator is the circle of the radius $w/2+2a$ (see section 3.4). If, however, the molecule is composed of two different in size or material resonators then the description of supermodes using only two sub-indices becomes not sufficient and one has to use four sub-indices.

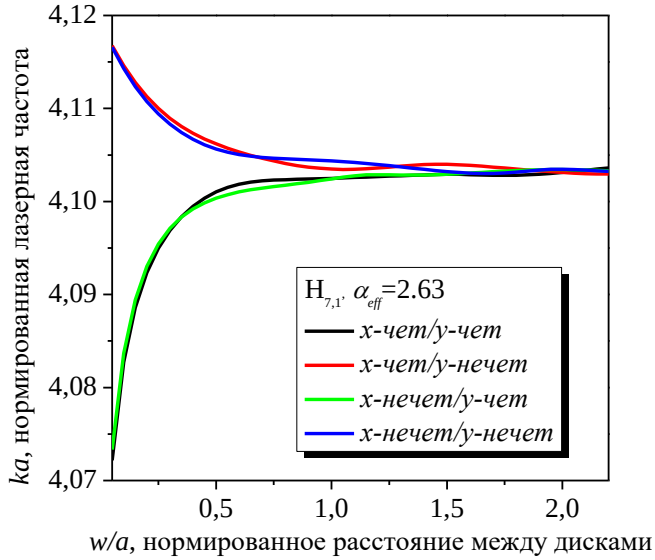

Fig. 4.4 Dependences of the normalized lasing frequencies of four supermodes $H_{7,1}^{(2)e,e}$, $H_{7,1}^{(2)e,o}$, $H_{7,1}^{(2)o,e}$, $H_{7,1}^{(2)o,o}$ in the twin-active-disk photonic molecule on the normalized rim-to-rim distance, $\alpha_{eff}=2.63$

When looking numerically for the roots of determinantal equations corresponding to the matrix equations (4.18) – (4.21), the initial guesses were taken as the eigenvalues of the modes $H_{m.n}$ in the stand-alone circular resonator.

Analysis shows that if $w < a$, then the quartet of supermodes form two pairs of modes with close frequencies. However, the most interesting phenomenon is that the thresholds of lasing of supermodes of all classes can be both lower and higher than for the corresponding mode of the stand-alone resonator. The lowering of thresholds is more pronounced for the *y*-odd supermodes.

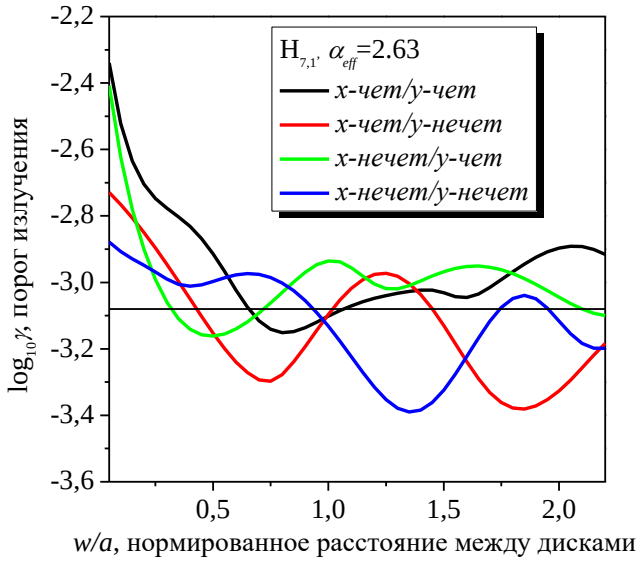

Fig. 4.5 The same as in Fig. 4.4, however for the lasing thresholds. The straight line shows the threshold of the mode $H_{7,1}$ in the stand-alone disk resonator, $\alpha_{eff} = 2.63$

In Fig. 4.6, we present the near fields for the four supermodes $H_{7,1}^{(2)e,e}$, $H_{7,1}^{(2)e,o}$, $H_{7,1}^{(2)o,e}$, $H_{7,1}^{(2)o,o}$ in the twin-active-disk photonic molecule. Note that the fields of the even across the *y*-axis supermodes show a stronger leakage to the air gap between the disks and therefore have a smaller overlap with the active region. As a result, their thresholds become much higher, at $w \to 0$, than the thresholds of the *y*-odd supermodes (see Fig. 4.5).

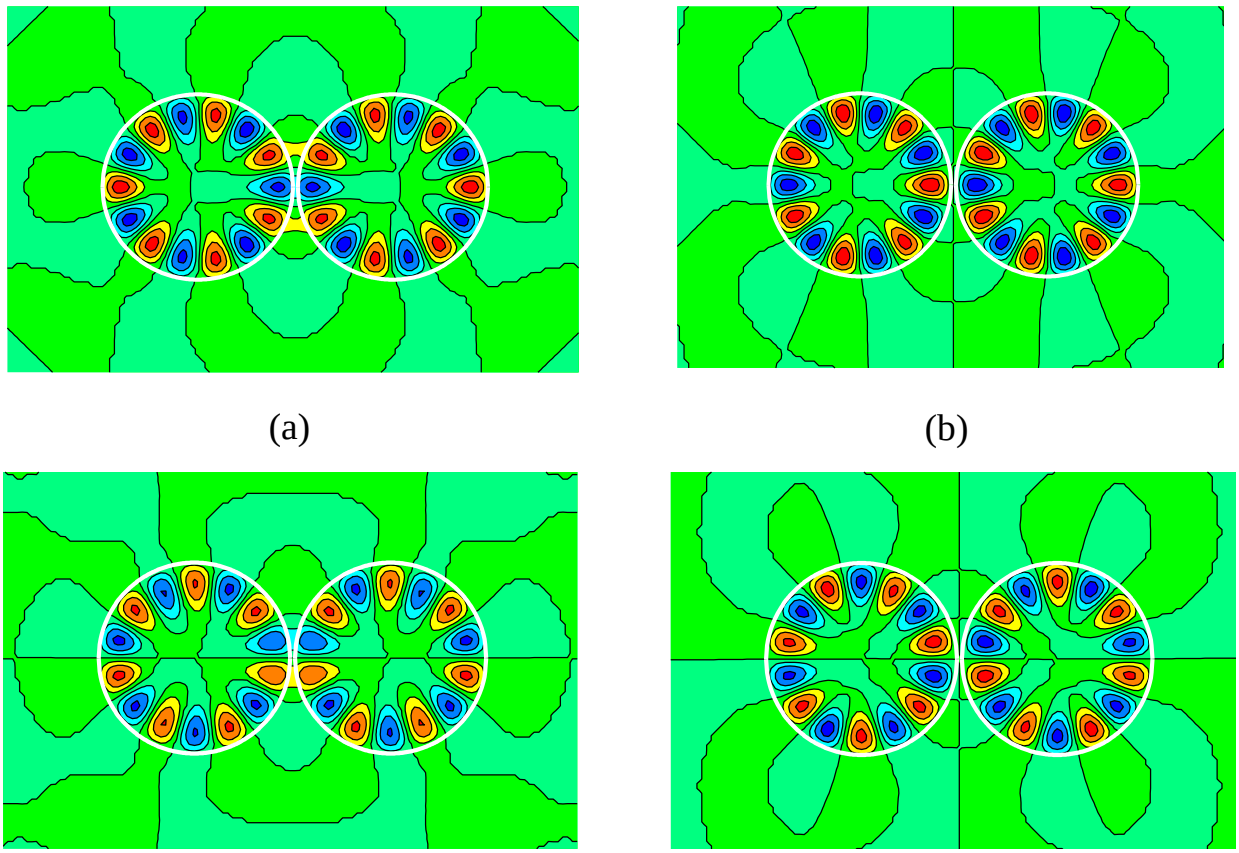

(a) (b)

(c) (d)

Fig. 4.6 Near H-fields (lines $H_z = const$) of the four relative supermodes in a twin-active-disk photonic molecule: (a) $H_{7,1}^{(2)e,e}$ x-even/y-odd, (b) $H_{7,1}^{(2)e,o}$ x-even/y-odd, (c) $H_{7,1}^{(2)o,e}$ x-odd/y-even, (d) $H_{7,1}^{(2)o,o}$ x-odd/y-odd. Red and blue colors represent the field spots with opposite phase, $w/a = 0.01$

The expression for the field of the photonic molecule laser in the far zone can be obtained using the large-argument asymptotics for the Hankel functions [156],

$$U(\rho,\varphi) \sim \sqrt{\frac{2}{i\pi k\rho}} e^{ik\rho}\Phi(\varphi) + \bar{o}\left(1/\rho\right), \qquad \rho \to \infty, \tag{4.22}$$

where the function $\Phi(\varphi)$ characterizes the dependence of the radiated field on the angle $\varphi = \arctan(y/x)$ in the plane of resonators and is usually called the radiation pattern,

$$\Phi(\varphi)=\sum_{p=-\infty}^{\infty}(-i)^p\left[C_p e^{-ik\frac{\rho_{12}}{2}\cos\varphi}+D_p e^{ik\frac{\rho_{12}}{2}\cos\varphi}\right]e^{ip\varphi}. \qquad (4.23)$$

In the case of two identical resonators, $\Phi(\varphi)$ can be written separately for each of the symmetry classes depending on the parity properties across the *x* and *y*-axes,

$$\Phi(\varphi)=\sum_{p=0(1)}^{\infty}\mu_p(-i)^p\left[C_p\pm(-1)^p D_p\right]\left[e^{-ik\frac{\rho_{12}}{2}\cos\varphi}\pm(-1)^p e^{ik\frac{\rho_{12}}{2}\cos\varphi}\right]S_p(\varphi) \qquad (4.24)$$

where $\mu_p=1/2$ if $p=0$ and $\mu_p=1$ if $p\neq 0$; $S_p(\varphi)=\cos p\varphi$ or $\sin p\varphi$ is chosen in dependence of the parity across the *x*-axis. The sign «+» corresponds to the families *x*-even/*y*-even and *x*-odd/*y*-odd and the sign «-» corresponds to the families *x*-even/*y*-odd and *x*-odd/*y*-even.

The directionality of the emission of each of the supermodes can be conveniently characterized with the aid of the quantity borrowed from the antenna theory and known as *directivity*,

$$D=\frac{2\pi}{P}|\Phi(\varphi_0)|^2, \qquad P=\int_0^{2\pi}|\Phi(\varphi)|^2\,d\varphi, \qquad (4.25)$$

where φ_0 is the angle of radiation of the most intensive of the radiation pattern beams, and *P* is, within a constant, the full power radiated by the given mode.

In Fig. 4.7, we demonstrate the dependences of the directivity and the angle of orientation of the main beam in the first quadrant of the (x,y)-plane on the normalized rim-to-rim distance *w/a*, for the supermodes $H_{7,1}^{e,e}, H_{7,1}^{e,o}, H_{7,1}^{o,e}, H_{7,1}^{o,o}$ of the four mentioned above classes of symmetry. Here, one should be reminded that the omnidirectional radiation has the directivity *D*=1, and for any mode of the stand-alone circular resonator (having the radiation pattern $\Phi(\varphi)=\cos m\varphi$ or $\sin m\varphi$) we obtain *D*=2.

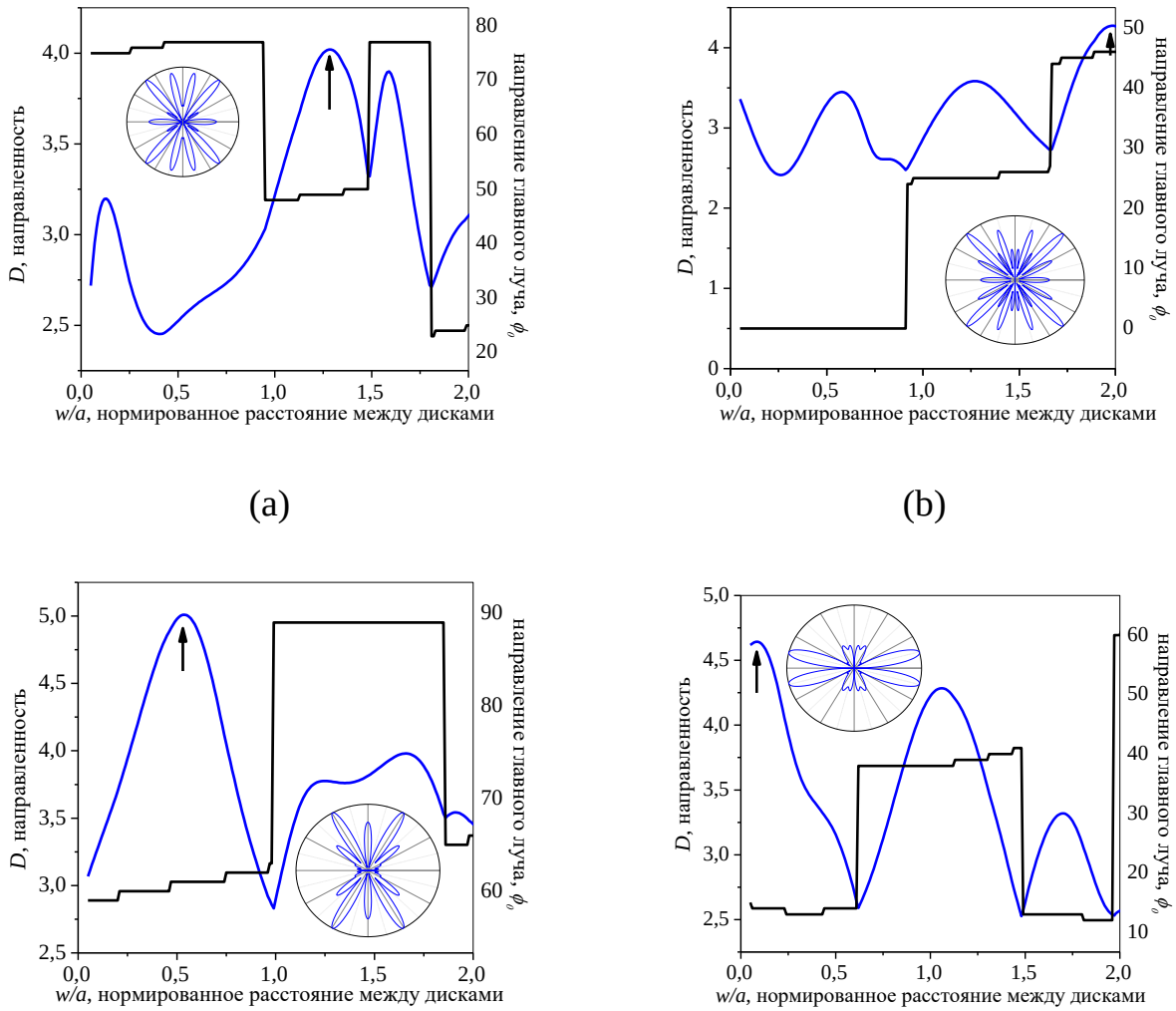

Fig. 4.7 The directivities of emission and the angles of maximum radiation as a function of the rim-to-rim distance for four supermodes (a) $H_{7,1}^{(2)e,e}$, x-even/y-even, (b) $H_{7,1}^{(2)e,o}$, x-even/y-odd, (c) $H_{7,1}^{(2)o,e}$, x-odd/y-even, and (d) $H_{7,1}^{(2)o,o}$, x-odd/y-odd

Thus, the optical coupling of two active resonators enables one to improve the directionality of emission. As one can see from the plots in Fig. 4.7, the angle of orientation of the main beam experiences finite jumps at certain values of the rim-to-rim distance. This is explained by the fact that when this distance varies, each of the beams of radiation pattern varies continuously in the amplitude and orientation and the role of the main beam may be transferred from one beam to another.

The insets in Fig. 4.7 show the normalized radiation patterns for the relative whispering-gallery supermodes of the four symmetry classes in the twin photonic

molecule. The corresponding rim-to-rim distances provide maximum directivities in each case and are marked with arrows. They demonstrate that, thanks to the two-fold symmetry, usually there are four identical main beams of the far-field radiation pattern, or one in each quadrant. However sometimes they merge together and form two main beams directed along one of the symmetry lines.

Therefore at the points of jumps on the dependences of the main-beam orientation on the rim-to-rim distance the number of identical main beams is always eight or four. Note that the supermodes of the class *x*-odd/*y*-odd cannot have less that four main beams and therefore show generally smaller values of directivity than the supermodes of the other symmetry classes.

4.2. Whispering-gallery supermodes in cyclic photonic molecules

Photonic molecules may have wide variety of configurations however the most interesting properties are associated with those of them whose structure is somehow ordered. Among such structures, there are cyclic photonic molecules that have a cyclic symmetry: the molecule having M elements repeats itself after the rotation by the angle π/M relatively to some point (the center). Two-dimensional model of the cyclic photonic molecule built of eight circular resonators is depicted in Fig. 4.8.

As usually, we will assume that in the pump-off regime the bulk refractive index of the resonators material is α. After the transfer to the 2-D model, this value is replaced with the effective refractive index, see section 2.1. Under the pumping it takes complex value, $\nu = \alpha_{eff} - i\gamma$.

As the centers of the resonators are located in the vertices of the regular polygon of the M -the order, the rim-to-rim distance, $w > 0$, is the same for any pair of adjacent resonators. Therefore, besides of the cyclic (i.e. rotational) symmetry, a cyclic photonic molecule of circular resonators possesses M lines of the mirror symmetry. Each symmetry line goes through the polygon center and also connects either its opposite vertices and opposite median points (if M is even) or the vertices with the opposite median points (if M is odd).

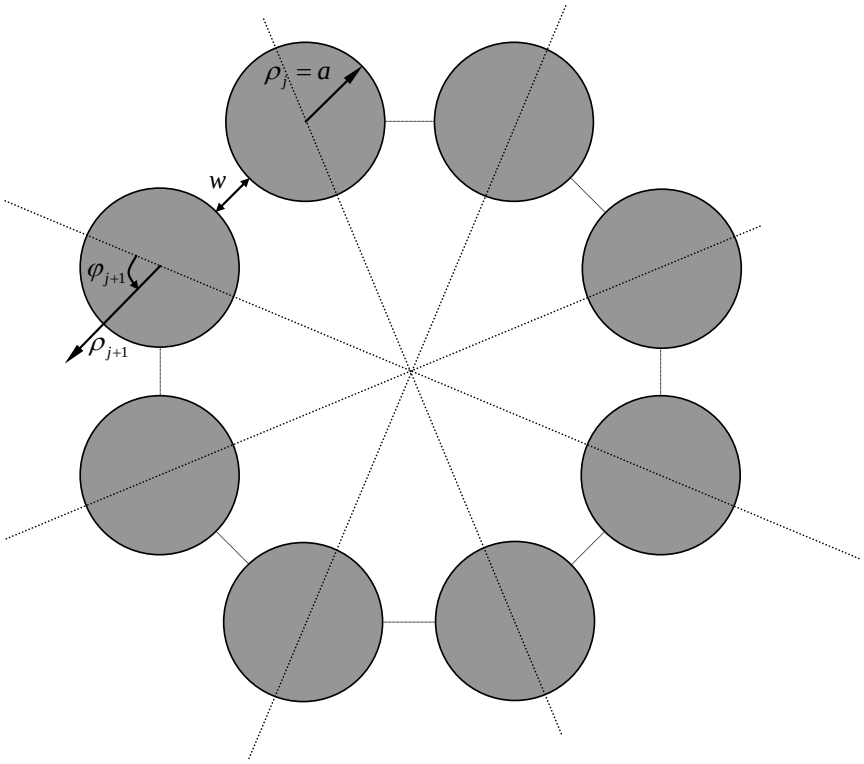

Fig. 4.8 Two-dimensional model of a cyclic photonic molecule made of M = 8 optically coupled active circular resonators

In view of the mentioned geometrical properties, all supermodes of a cyclic photonic molecule split into orthogonal classes according to the field symmetry. These symmetry classes have been discussed in details in [165]. The number of classes and the degeneracy of modes depends on the parity of the number M of the elementary resonators in a cyclic photonic molecule.

For a cyclic photonic molecule composed of circular cavities, the lasing eigenvalue problem (2.8), (2.12) – (2.13), (2.15) can be treated with the aid of the partial separation of variables and addition theorems for cylindrical function, similarly to the twin-molecule case (see section 4.1). Here we need M local polar coordinates corresponding to the number of elementary resonators. Each local coordinate system is introduced in the following manner: the origin of the j-the polar coordinates (ρ_j, φ_j) is taken in the center of the j-the resonator and the angle

φ_j is counted counter-clockwise from the line of symmetry passing through the resonator center (see Fig. 4.8).

As before in this Chapter, we will consider the case of the H-polarization only. Expand the function $U = H_z$ as a series in terms of the trigonometric functions of the local angle φ_j inside of every elementary circular resonator. Here, according to the condition of the local power finiteness, we use only the Bessel functions in the coefficients of the series as functions of local radial coordinate, ρ_j. We can also take into account the symmetry or anti-symmetry of the field function across the symmetry line passing through its center by choosing the sin or cos trigonometric functions, respectively. Outside of all resonators, we present the field function as a linear combination (a sum) of the similar series but with only the Hankel functions in the coefficients, to satisfy the radiation condition at infinity,

$$\begin{aligned} &\rho_j < a, \quad j = 1,...M, \qquad U(\rho_j,\varphi_j) = \sum_{p=(0)1}^{\infty} A_p^j J_p(k\nu\rho_j) S_p(\varphi_j) \\ &\sum_{j=1,...M} \{\rho_j > a\}, \qquad U(\rho,\varphi) = \sum_{j=1}^{M} \sum_{p=(0)1}^{\infty} B_p^j H_p^{(1)}(k\rho_j) S_p(\varphi_j) \end{aligned} \tag{4.26}$$

where $S_p(\varphi_j) = \cos p\varphi_j$ or $\sin p\varphi_j$, k is the free-space wavenumber, $\left\{A_p^j, B_p^j\right\}_{p=(0)1}^{\infty}$ are M infinite sequences ($j = 1,...M$) of unknown coefficients of the field expansions in the local polar coordinates. Further, substituting (4.26) into the boundary conditions (2.12), using the addition theorems for cylindrical functions, and making algebraic transformations similarly to section 4.1, we obtain the following block-type ($M\times M$) infinite-matrix equation:

$$x_m^j + \sum_{\substack{s=1 \\ s\neq j}}^{M} \sum_{p=(0)1}^{\infty} (-1)^m \mu_p \frac{J_m(\kappa) V_p(\kappa,\gamma)}{F_p(\kappa,\gamma) J_p(\kappa)} K_{mp}^{js(\pm)} x_p^s = 0, \tag{4.27}$$

where $m = (0)1, 2, ...$, $j = 1,...M$, $\kappa = ka$,

$$K_{mp}^{js(\pm)} = [(-1)^p H_{m-p}^{(1)}(k\rho_{js})\cos(p\theta_{js}^{+} - m\theta_{js}^{-}) \pm H_{m+p}^{(1)}(k\rho_{js})\cos(p\theta_{js}^{+} + m\theta_{js}^{-})], \quad (4.28)$$

$$x_m^j = A_m^j F_m(\kappa,\gamma) J_m(\kappa), \quad (4.29)$$

and the functions $F_p(\kappa,\gamma)$ and $V_p(\kappa,\gamma)$ are defined by (4.5). The coefficient $\mu_p = 1/2$ if $p = 0$ or $\mu_p = 1$ if $p \neq 0$. For $K_{mp}^{js(\pm)}$ in (4.28) we take the sign «+» if in (4.26) $S_p(\varphi_j) = \cos p\varphi_j$ and the sign «-» if $S_p(\varphi_j) = \sin p\varphi_j$. The distance ρ_{js} between the centers of the j-th and the s-th resonators is determined as follows:

$$\rho_{js} = \frac{2a + w}{\sin(\pi / M)} \sin(|j - s|\pi / M) \quad (4.30)$$

The angles θ_{js}^{+} and θ_{js}^{-} are determined from

$$\theta_{js}^{+} = \frac{M\pi + |j - s|2\pi}{2M}, \quad \theta_{js}^{-} = \frac{M\pi - |j - s|2\pi}{2M}. \quad (4.31)$$

Note that equation (4.27) has the structure analogous to that of equation (4.8) of the previous section. A study of its coefficients reveals that it generates a canonical Fredholm operator in the space of the number sequences l_2, provided that all $\rho_{js} > 2a, \quad j \neq s$. Then, its characteristic numbers can be approximated with the characteristic numbers of the truncated counterpart, i.e. by the zeros of its finite-order determinant. Therefore, the elementary resonators in the cyclic photonic molecule should not touch each other.

Now, coming back to the symmetry classes of modes we will write explicitly two matrix equations for the most interesting classes. The first is the class of modes $H_{m,n}^{(M)all-even}$, whose fields are even with respect to all existing symmetry lines in the cyclic photonic molecule. The second class is for the modes $H_{m,n}^{(M)all-odd}$, whose fields

are odd with respect to all existing lines of symmetry. For the modes of these two symmetry classes, the field expansion coefficients in neighboring resonators (in the corresponding local coordinates) are connected by the relations

$$A_p^s = A_p^{s+1}, \quad x_p^s = x_p^{s+1} \tag{4.32}$$

On substituting (4.32) into (4.27), we obtain the needed matrix equations where, without a loss of generality, we may fix the resonator number j equal to 1,

$$x_m^1 + \sum_{p=0(1)}^{\infty} (-1)^m \mu_p \frac{J_m(\kappa)V_p(\kappa,\gamma)}{F_p(\kappa,\gamma)J_p(\kappa)} \left[\sum_{s=2}^{M} K_{mp}^{1s(\pm)} \right] x_p^1 = 0, \tag{4.33}$$

and in $K_{mp}^{1s(\pm)}$ we take the sign «+» for the modes of the "all-even" class and the sign «-» for the modes of the "all-odd" class. If M=2, then the equation (4.33) coincides with the equations (4.18)-(4.21) of section 4.1.

A numerical search for the eigenvalues, (κ,γ), of each class is reduced to solving the corresponding determinantal equation generated by the matrix (4.33). If we denote the order of truncation of this matrix as N, then the convergence, with $N \to \infty$, of the approximate numerical solution to the solution of the infinite-dimension determinantal equation is guaranteed. This follows from the fact that (4.33) is a Fredholm second kind operator equation (see (4.12), section 4.1) for the number sequences of the space l_2. In the process of computations, we have fixed the accuracy of the numerical solution of determinantal equations by the secant method at the level of 10^{-7}.

The aim of our numerical analysis was the frequencies and thresholds of lasing of the supermodes $H_{7,1}^{(M)all-even}$ and $H_{7,1}^{(M)all-odd}$ belonging to the mentioned above two symmetry classes. In this section, we present the results computed for the supermodes built on the whispering-gallery modes inside each of the elementary circular resonators.

In the computations, the order of truncation of the determinant, N, was established in such a way that the eigenvalues (κ^N, γ^N) were differing from the same eigenvalues, $(\kappa^{2N}, \gamma^{2N})$, found from the solution of the determinant truncated at $2N$, at the level of 10^{-5}. To follow this rule, it has been empirically found that for the supermodes $H_{7,1}^{(M)all-even}$ and $H_{7,1}^{(M)all-odd}$ one can take $N \approx 45$.

In Fig. 4.9, presented are the dependences of the lasing frequencies of the supermodes (for M=2,3,4,5,6) of the two indicated classes of symmetry on the normalized rim-to-rim distance, w/a. Here all curves going up at $w/a \to 0$, are for the whispering-gallery supermodes of the class $H_{7,1}^{(M)all-even}$ (which demonstrate a blue shift in frequency), and those going down at $w/a \to 0$ are for the supermodes $H_{7,1}^{(M)all-odd}$ (a red shift). A noticeable difference in frequency between the supermodes of these two classes is observed only if $w < a$, and the frequencies weakly depend on the number of elementary cavities, M. If, contrary, $w > a$, then these supermodes are nearly degenerate in frequency. As for the thresholds of lasing, they are much more sensible to the number of resonators and the separation between them, even if $w > a$.

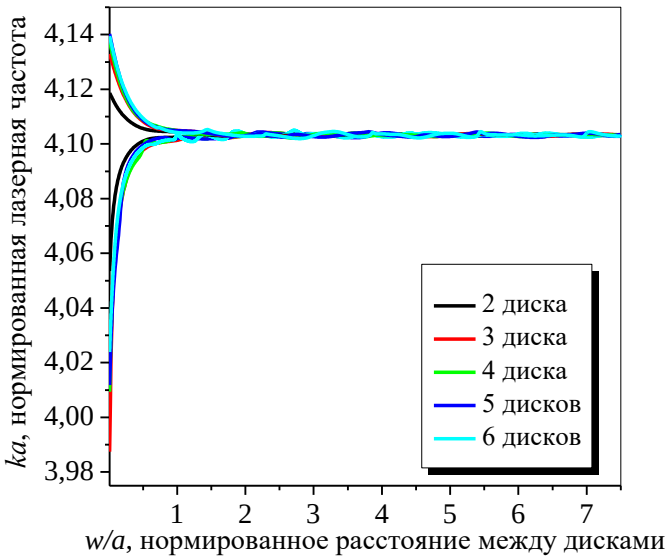

Fig. 4.9 Dependences of the lasing frequencies of the supermodes $H_{7,1}^{(M)all-even/odd}$ in the cyclic photonic molecules of M active circular disks on the rim-to-rim distance

In Figs. 4.10 and 4.11, presented are the dependences of the lasing thresholds of the same supermodes of two classes of symmetry, $H_{7,1}^{(M)all-even}$ and $H_{7,1}^{(M)all-odd}$, for different *M*, on the rim-to-rim distance normalized to the radius *a*.

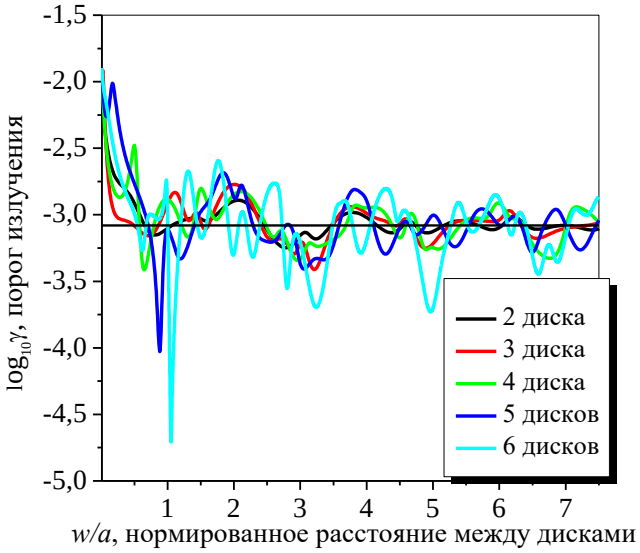

Fig. 4.10 Lasing thresholds of the supermodes $H_{7,1}^{(M)all-even}$ in the cyclic photonic molecule as a function of the normalized rim-to-rim distance. The straight line shows the threshold of the mode $H_{7,1}$ in the stand-alone circular cavity. $\alpha_{eff} = 2.63$

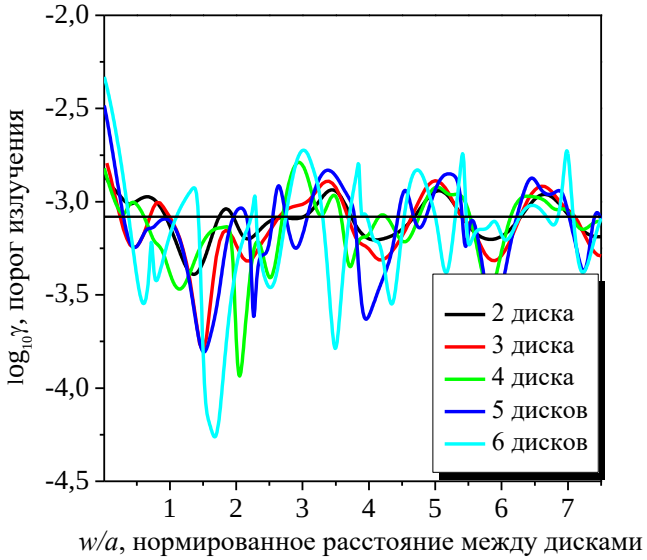

Fig. 4.11 The same as in Fig. 4.10, however for the supermodes $H_{7,1}^{(M)all-odd}$

It is visible that the lasing thresholds of the supermodes of the first class ("all-even modes") grow up much more rapidly if the elementary resonators get closer to each other $(w \to 0)$, than the mode of the second class ("all-odd modes"). This effect has been already discussed in section 4.1 for the twin-disk molecule. It is explained by the fact that the anti-symmetry prevents the modes of the second class from being pushed out from the disks, i.e. from the active region. The modes of the first class display so strong coupling at small *w* that their field spots can merge together.

The most important and promising result found in the analysis of the whispering-gallery supermodes is they can have much lower thresholds of lasing than the corresponding whispering-gallery mode in a stand-alone circular cavity. This effect is observed for the supermodes of all classes of symmetry (see Figs. 4.10 and 4.11) however in the narrow bands of the parameter *w/a* variation. As visible from these plots, it needs a fine tuning of the rim-to-rim distance to the optimal value. At the same time, one can see that if the number of elementary resonators, *M,* is taken larger then the discovered resonant drop of the lasing threshold becomes deeper.

Here, it is interesting to remind that a similar effect had been predicted in 1996 by one of the pioneers of semiconductor lasers, Nick Holonyak. It was done in the course of fabrication and experimental investigation of the probably first ever cyclic-photonic-molecule lasers shaped as six active ring resonators placed on a substrate [89]. The authors of that paper, however, had admitted that they expectation was not fulfilled and instead of threshold reduction they had found its growth, in two times, in comparison to the solitary ring resonator. Our simulations enable us to suggest that the rim-to-rim distance chosen in [89] happened to be wrong. This is not a surprise as the optimal separation is rather large, between *a* and 2*a*, and must be tuned with accuracy up to 0.1*a*. It can be expected that a more detail study of the microcavity lasers shaped as cyclic photonic molecules can lead to experimental discovery of the effect of the lasing threshold reduction for their supermodes.

In Fig. 4.12, we show the near field patterns of the supermodes $H_{7,1}^{(M)all-even}$ and $H_{7,1}^{(M)all-odd}$ in the photonic molecule laser made of $M = 6$ active circular cavities.

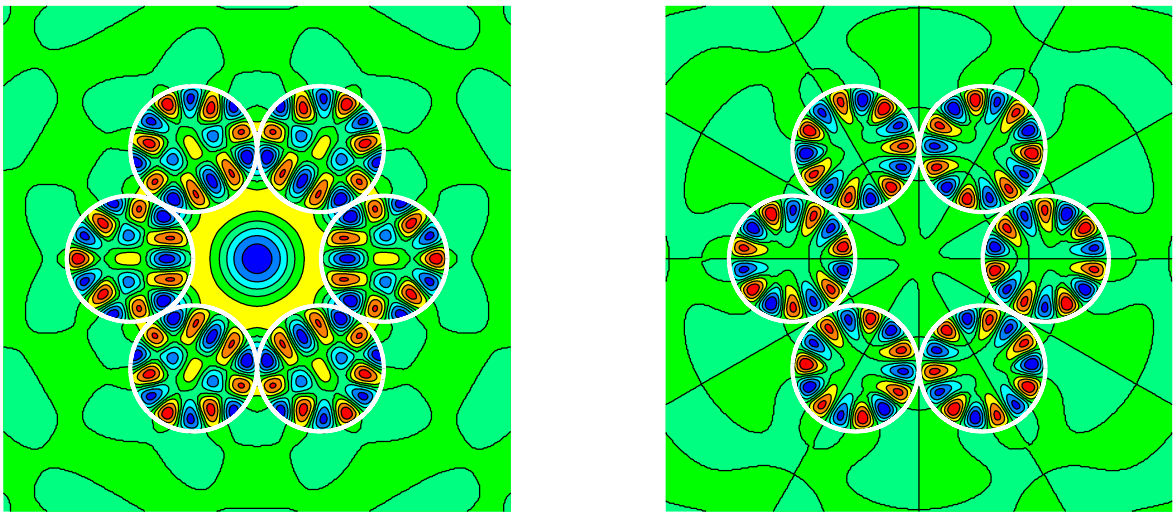

(a) (b)

Fig. 4.12 Near fields (lines $H_z = const$) of supermodes $H_{7,1}^{(M)all-even}$ (a) and $H_{7,1}^{(M)all-odd}$ (b) in the photonic molecule made of six disks with $w/a = 0.01;\ \alpha_{eff} = 2.63$

One may notice that the supermode of the first class has the field which leaks strongly (at the given rim-to-rim distance, w) into the filled with the air inner domain of the cyclic photonic molecule that the field of the second class. The amplitude of the field in the center of the air space in Fig. 4.12 (a) is actually the same as in the hot spots of the whispering gallery field in the elementary dielectric cavities.

In accordance to the results obtained in section 3.4, such a pushing out of the field out of the disks reduces the overlap coefficient of the active region with the electric field of the first supermode and hence must lead to the growth of its threshold of lasing. Indeed, a comparison of the thresholds at the separation $w/a = 0.01$ on the corresponding curves in Figs. 4.10 and 4.11 reveals that the values of $\gamma_{7,1}^{(M)all-even}$ and $\gamma_{7,1}^{(M)all-odd}$ differ by an order of magnitude.

It should be noted, for generality, that besides of the studied here supermodes of the partial regions having large refractive index, in the cyclic photonic molecules may exist, in principle, the supermodes of the inner air-filled region. Their fields are concentrated mainly in the center of molecule and have a bad overlap with the active region. Therefore, in view of the results of section 3.4, we may predict that their thresholds of lasing are very high.

4.3. Supermodes built on the monopole and dipole modes

In this section, we will present and discuss the numerical study results related to the supermodes of the cyclic photonic molecules built on the lowest-type modes in the elementary circular resonators: monopole modes (H_{01}) and dipole modes (H_{11}). As it has been shown in section 2.3, it means that the diameters of the elementary disks are smaller than the free-space wavelength, λ. For example, if the disk has effective refractive index $\alpha_{eff} = 2.63$, then the lowest lasing modes have the normalized to radius eigenfrequencies $\kappa_{01}^{H} = 0.8838$ and $\kappa_{11}^{H} = 1.405$. As here $\kappa = ka$, this means that the corresponding values of diameters are $2a_{01} = 0.281\lambda$ и $2a_{11} = 0.447\lambda$. It should be also reminded that the dipole mode is twice degenerate in a stand-alone circular resonator, and the monopole mode is not degenerate.

The associated thresholds of lasing of the monopole and dipo,e modes in a stand-alone cavity are much higher than the thresholds of the whispering-gallery modes (see section 2.3). For the mentioned above disk with $\alpha_{eff} = 2.63$ they are $\gamma_{01}^{H} = 0.3595$ and $\gamma_{11}^{H} = 0.275$, respectively. However these thresholds can be lowered using the optical coupling between the resonators, for example, by building a cyclic photonic molecule of several sub-wavelength disks.

As mentioned in the preceding section, all supermodes of a cyclic photonic molecule split to orthogonal classes in dependence of the parity of their fields across the existing lines of symmetry. The number of such classes depends on the value and parity of the number of elementary circular cavities, *M*. Consider the class of symmetry “even-odd”, for which the field inside every elementary resonator is symmetric across the line going through its center and molecule’s center however is anti-symmetric across the line going through the median point of the air gap between the adjacent disks and molecule’s center. In other words, the supermode field of this class repeats itself in the absolute value after the rotation by π / M however changes the sign (or the phase). Then, similarly to the preceding section, the coefficients of the field expansions in the adjacent resonators are connected by the relation as

$$A_p^s = A_p^{s+1}, \quad x_p^s = x_p^{s+1}. \tag{4.34}$$

This relation should be substituted to (4.27). As the resonator number in a cyclic molecule, j, can be chosen arbitrarily, we can take, for convenience, $j=1$. Then, for the "even/odd" mode class we obtain the following matrix equation:

$$x_m^1 + \sum_{p=0(1)}^{\infty} (-1)^m \mu_p \frac{J_m(\kappa)V_p(\kappa,\gamma)}{F_p(\kappa,\gamma)J_p(\kappa)}\left[\sum_{s=2}^{M}(-1)^{s-1}K_{mp}^{1s(+)}\right]x_p^1 = 0, \tag{4.35}$$

where the coefficients $K_{mp}^{1s(+)}$ are given by (4.28) where one must take the sign «+» (as the field is even across the lines of symmetry going through the resonators centers). It should be stressed that this class of symmetry exists only in the cyclic configurations consisting of the even number of resonators, $M = 2M'$ [165].

We have searched for the lasing eigenvalues (κ,γ) numerically, by solving the determinantal equation generated by the matrix of (4.35) and truncated to finite order, *N*. here, it has been found empirically that for computing the eigenvalues of the supermodes $H_{0,1}^{(M)even-odd}$ and $H_{1,1}^{(M)even-odd}$ with the accuracy of 10^{-5} , one has to take the truncation number as $N \approx 25$. In Figs. 4.13 and 4.14, we present the dependences of the normalized frequencies and the thresholds of lasing, respectively, of the supermodes $H_{0,1}^{(M)even-odd}$ in the cyclic photonic molecules with *M* = 2,4,6,8,10 on the normalized rim-to-rim distance between the sub-wavelength disks, w/a. One can see that for any number *M* the frequencies grow up if the inter-disk spacing reduces (at $w \to 0$) and tend to the value of the frequency of the monopole mode $H_{0,1}$ in a stand-alone circular resonator, which is $\kappa_{0,1}^H = 0.8838$.

In contrast, the lasing thresholds of the monopole-type supermodes $H_{0,1}^{(M)even-odd}$ monotonically decrease if either the inter-disk spacing gets smaller or the number of elementary resonators, *M*, gets larger. If $w = 0.01a$, the threshold of this supermode

in the cyclic molecule made of six disks is by the order of magnitude lower than for the monopole mode $H_{0,1}$ in a stand-alone sub-wavelength cavity that is $\gamma_{0,1}^{H} = 0.3595$.

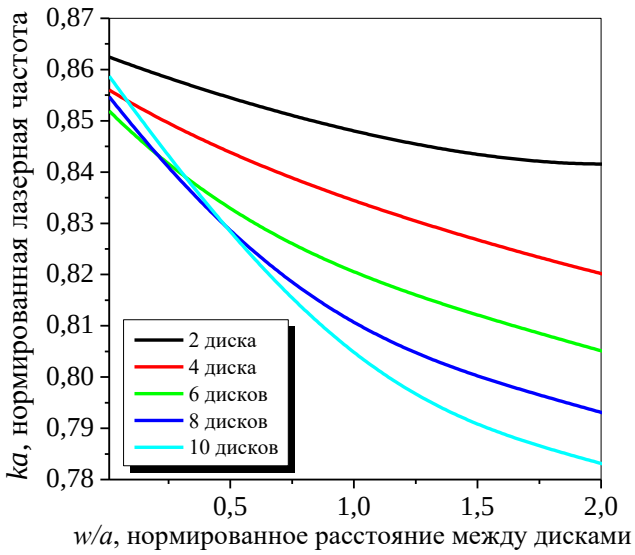

Fig. 4.13 Dependences of the frequencies of lasing for the monopole-type supermodes $H_{0,1}^{(M)even-odd}$ in the cyclic photonic molecules made of active sub-wavelength disks on the normalized rim-to-rim separation; $\alpha_{eff} = 2.63$

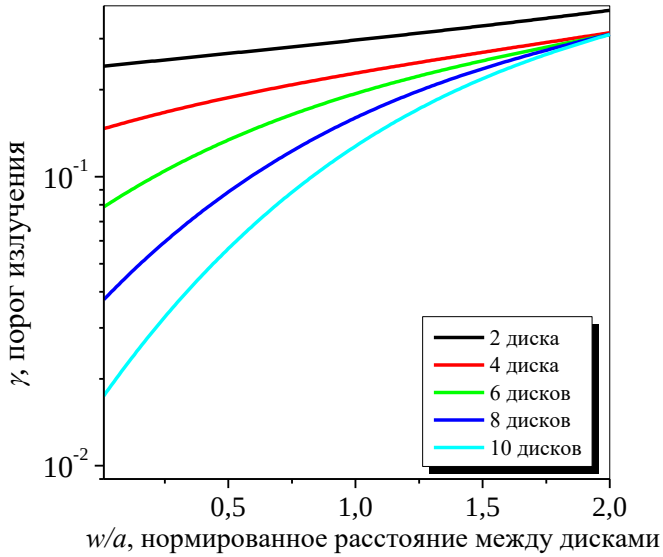

Fig. 4.14 The same as in Fig. 4. 13 however for the thresholds of lasing

In Figs. 4.15 and 4.16, we present the dependences of the normalized frequencies of lasing of the dipole-type supermodes $H_{1,1}^{(M)even-odd}$ of the same "even-odd" class as in the previous example on the normalized rim-to-rim distance, w/a. Here the number of disks in the cyclic photonic molecule is M = 2,4,6,8 and10.

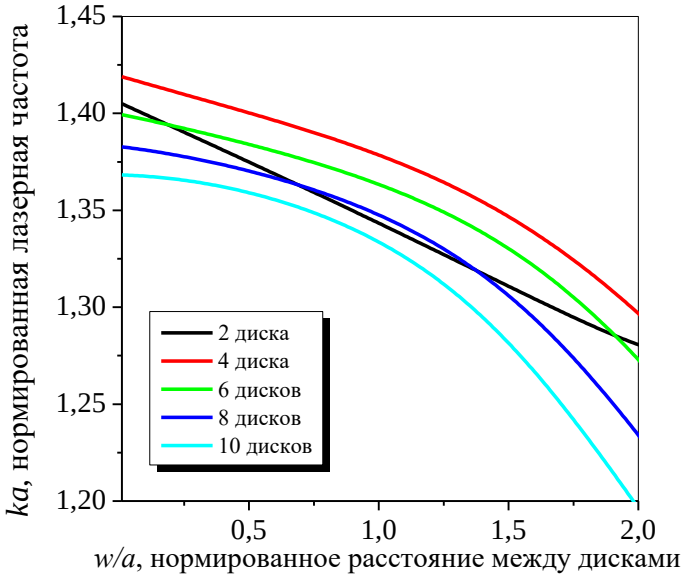

Fig. 4.15 Dependences of the frequencies of lasing for the dipole-type supermodes $H_{1,1}^{(M)even-odd}$ on the normalized rim-to-rim separation; $\alpha_{eff} = 2.63$

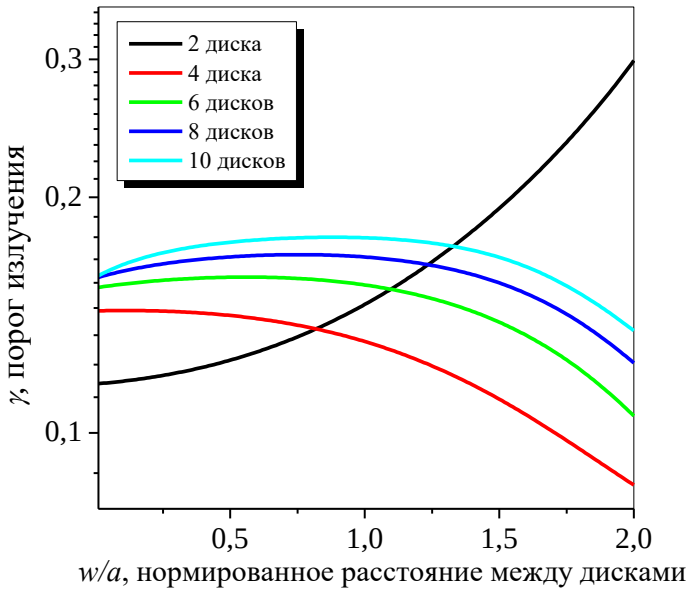

Fig. 4.16 The same as in Fig. 4. 15 however for the thresholds of lasing

As visible, for any number *M* the frequencies grow up if the inter-disk spacing decreases (at $w \to 0$) and approach to the frequency of the dipole mode $H_{1,1}$ in a stand-alone cavity, that is $\kappa_{1,1}^{H} = 1.405$ if refractive index is $\alpha_{eff} = 2.63$.

However, unlike the monopole-type supermode of the same class of symmetry, the thresholds of lasing of the dipole-type supermodes $H_{1,1}^{(M)even-odd}$ remain high if the inter-disk spacing, *w*, decreases, and even grow up if the number of elementary resonators, *M*, is taken greater. If $w = 0.01a$, then the threshold of lasing of this supermode in the cyclic photonic molecule made of six disks is almost twice higher than of the mode $H_{1,1}$ in a stand-alone cavity, that is $\gamma_{1,1}^{H} = 0.275$ (see section 2.3). An exception from this rule is the behavior of the supermode $H_{1,1}^{(2)even-odd}$ in a twin-active-disk molecule, whose threshold of lasing monotonically decreases if the inter-disk spacing *w* gets smaller

Still however, the dipole mode $H_{1,1}$ in a stand-alone circular dielectric resonator is known to be double degenerated (as well as all non-monopole modes). The degenerate modes have mutually orthogonal orientations of their fields and hence differ by their parity relatively to the origin of the azimuth coordinate. Therefore in the cyclic photonic molecule built of *M* identical circular resonators, besides of the already considered supermode $H_{1,1}^{(M)even-odd}$, there exists its sister-mode $H_{1,1}^{(M)all-odd}$ also built on the dipole-type modes in the elementary sub-wavelength cavities. It belongs to the other class of symmetry, “odd-odd or all-odd” as its field is anti-symmetric to all existing lines of symmetry in molecule. The corresponding to that class determinantal equation is generated by the matrix (4.33) in whose elements one has to take the coefficients $K_{mp}^{1s(-)}$.

In Figs. 4.17 and 4.18, presented are the dependences of the normalized frequencies and the thresholds of lasing, respectively, of the dipole-type supermodes $H_{1,1}^{(M)all-odd}$ of the class “odd-odd” in the cyclic photonic molecules having *M* = 2,4,6,8 and 10 elementary microdisk cavities on the normalized rim-to-rim distance between the disks, w/a.

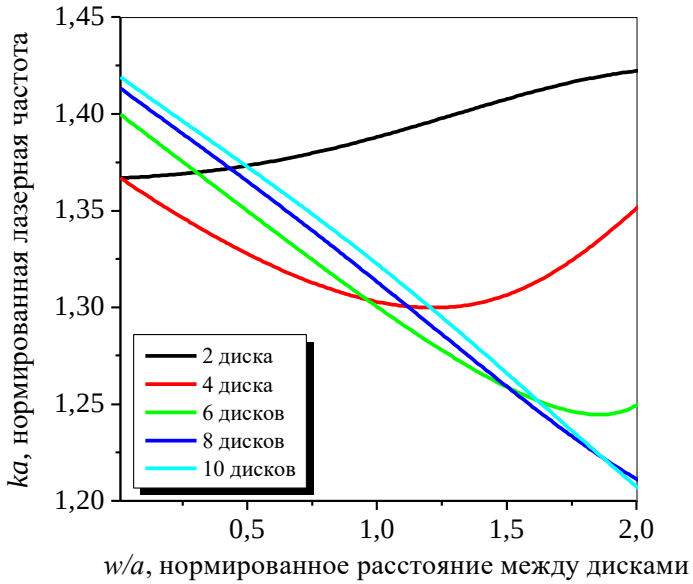

Fig. 4.17 Dependences of the frequencies of lasing for the dipole-type supermodes $H_{1,1}^{(M)all-odd}$ on the normalized rim-to-rim separation; $\alpha_{eff} = 2.63$

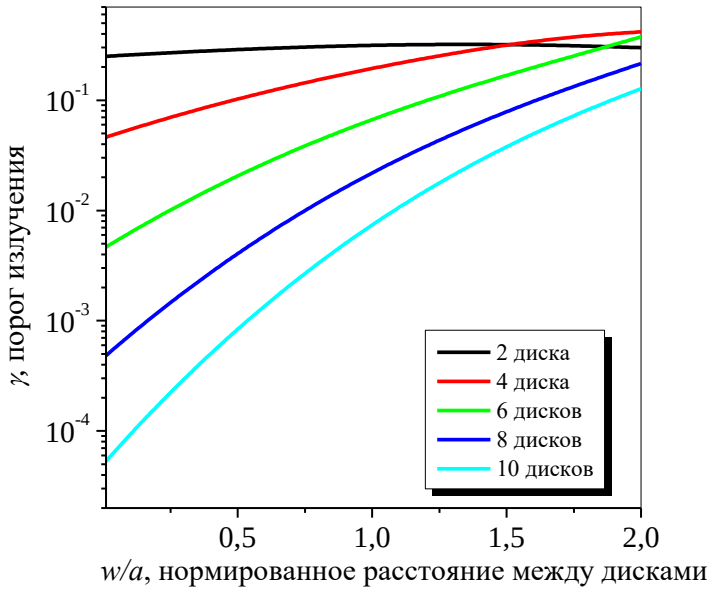

Fig. 4.18 The same as in Fig. 4. 17 however for the thresholds of lasing

Similarly to the other supermodes studied earlier, the lasing frequencies of the dipole-type supermodes $H_{1,1}^{(M)all-odd}$ grow up, for any M, if the inter-disk separation decreases $(w \to 0)$. They approach the value of the normalized frequency of the

dipole mode $H_{1,1}$ in a stand-alone sub-wavelength circular cavity, that is $\kappa_{1,1}^{H}=1.405$ if $\alpha_{eff}=2.63$.

The most interesting finding is the fact that the thresholds of lasing of the dipole-type supermodes of the class "odd-odd" drop down both if the elementary resonators get closer ($w\to 0$) and if their number, *M*, gets larger. This is the same effect as revealed earlier for the monopole-type supermode $H_{0,1}^{(M)even-odd}$.

There are, however, two additional observation that is worth to emphasize. First, for dipole-type supermode $H_{1,1}^{(M)all-odd}$ this effect is much more pronounced. A comparison of the curves in Figs. 4.18 and 4.14 shows that if the number *M* is increased by 2, the threshold of lasing of the supermode $H_{1,1}^{(M)all-odd}$ in the cyclic photonic molecule with the rim-to-rim separations $w=0.01a$ drops by approximately an order of magnitude. This is twice more rapidly than for the monopole-type supermode $H_{0,1}^{(M)even-odd}$. This is naturally explained by the more efficient mutual cancellation of the fields radiated by the elementary resonators, in the far zone.

Second, unlike supermodes $H_{0,1}^{(M)even-odd}$ that imply that *M* is even, the dipole-type supermodes $H_{1,1}^{(M)all-odd}$ of the "odd-odd" class exist in the cyclic photonic molecules with any number *M* of elementary circular cavities, both even and odd.

In Fig. 4.19, we visualize the near fields of the monopole and the dipole-type supermodes of the symmetry class "even-odd", and also the dipole-type supermode of the class "odd-odd," in the cyclic photonic molecule made of ten active sub-wavelength circular cavities. A comparison of the fields in Figs. 4.19 (a) and (b) tells that the field of the "even-odd" dipole-type supermode leaks stronger to the outer space than the field of the monopole supermode of the same class. It results in the higher threshold of lasing (see Figs. 4.14 and 4.16). The field of the dipole-type supermode $H_{1,1}^{(M)all-odd}$ leaks much weaker (Fig. 4.19 (c)) than that of the $H_{1,1}^{(M)even-odd}$ supermode (Fig. 4.19 (b)). In this sense it behaves similarly to the field of the monopole-type supermode that entails the lower thresholds (see Figs. 4.16 and 4.18).

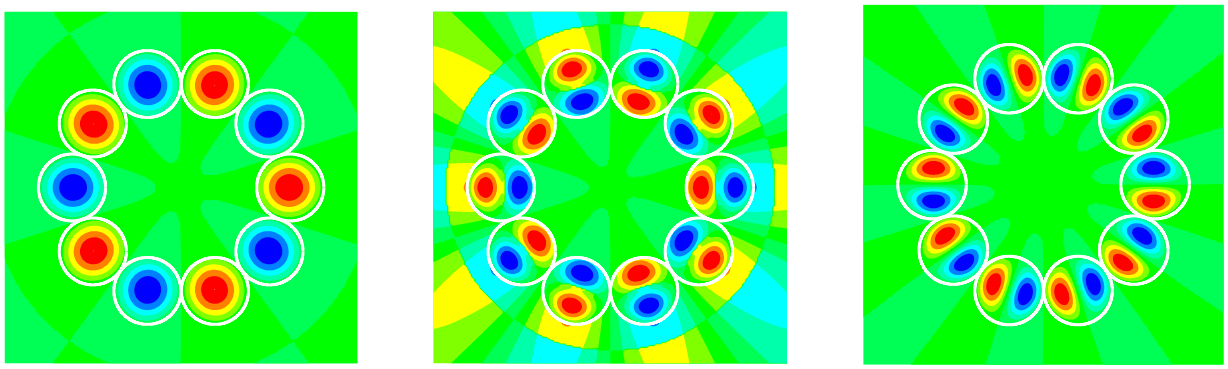

(a) (b) (c)

Fig. 4.19 Near fields (lines $H_z = const$) for the supermodes $H_{0,1}^{(M)even-odd}$ (a), $H_{1,1}^{(M)even-odd}$ (b) and $H_{1,1}^{(M)all-odd}$ (c) in the cyclic photonic molecule made of 10 active sub-wavelength circular cavities with rim-to-rim distance $w/a = 0.01$; $\alpha_{eff} = 2.63$

It is also worth noting that there exists a certain similarity between the structure and symmetry of the field of the monopole supermode $H_{0,1}^{(M)even-odd}$ in a cyclic photonic molecule and so-called π-type mode in a resonator of the electron-vacuum source of microwaves, the cavity magnetron [166].

Indeed, the cavity of the classical magnetron has a cyclic symmetry and M lines of mirror symmetry, and here M is always an even number. Therefore the field of the π-type mode has in fact a structure of the supermode and repeats itself in the absolute value if rotated in azimuth by π/M (i.e. in the adjacent side cavities) however changes the sign. We can suppose that the π-type mode of the magnetron cavity with M=6 or M=8 has the lowest ohmic losses thanks to the highest degree of anti-symmetry, and probably good overlap with the rotating electron cloud, which plays the role of active region in magnetron. As a result, the starting current for the π-type mode happens to be the smallest, similarly to the small threshold of lasing of the monopole-type supermode $H_{0,1}^{(M)even-odd}$ in a cyclic photonic molecule.

CONCLUSIONS FOR CHAPTER 4

In this Chapter, we have considered the 2-D models of the active cyclic photonic molecules composed of finite number of open circular dielectric resonators located in the vortices of a regular polygon. Such models have enabled us to investigate, using the lasing eigenvalue problem approach, the lasing spectra and thresholds of the natural modes of photonic molecules. The results of this study have been published in the journals [3–5] and conference proceedings [15–17, 23– 25, 28]; they lead to the following conclusions:

1. Natural modes of the cyclic photonic molecules are always “supermodes,” i.e. compound modes of the optically coupled partial regions: in our case, elementary circular resonators and air gaps. Besides, they split into finite number of orthogonal classes according to the symmetry of supermode fields. Therefore, to give them a complete nomenclature, it is necessary to introduce several integer indices characterizing the field variations inside every elementary resonator, and also the indices indicating the classes of symmetry.

2. Any supermode in a cyclic photonic molecule (built either on the whispering-gallery modes or on the monopole and dipole modes in the elementary resonators) can have the thresholds of lasing both higher and lower than the thresholds of the same modes in a stand-alone resonator. The values of the thresholds depend on the class of symmetry, rim-to-rim distance, and the number of the elementary resonators.

3. For the supermodes of all classes of symmetry built on the whispering-gallery modes, it is possible to considerably lower the threshold of lasing in comparison to the stand-alone resonator. This is a resonant effect requiring a fine tuning of the rim-to-rim distance with the accuracy of 0.1 of the disk radius. If the number of resonators in the molecule gets larger, the minimum of the threshold becomes deeper however its position changes.

4. For the supermodes of certain classes of symmetry built on the monopole and dipole modes in the elementary disks, one cal also lower the thresholds of lasing considerably in comparison to the stand-alone circular resonator. However this is non-resonant effect. The drop in the threshold becomes deeper if either the number of elementary resonators gets larger or the resonators are getting closer to each other. Adding a new resonator to a cyclic photonic molecule lowers the threshold of such supermodes by a half-order in magnitude, for the refractive index of 2.63.

5. A growth of the thresholds of lasing for the supermodes of the cyclic photonic molecules always corresponds to either a larger pulling of their fields into the central air-filled area of a cyclic molecule or to a stronger leakage to the outer space. This behavior of thresholds and mode fields can be explained using the Optical Theorem for the open resonators with partial active regions.